Effects of glassing matrix deuteration on the relaxation properties of hyperpolarized ^{13}C spins and free radical electrons at cryogenic temperatures

Christopher Parish (iD), Peter Niedbalski, Qing Wang, Fatemeh Khashami, Zahra Hayati, Mengtian Liu, Likai Song, and Lloyd Lumata (iD)

View Online   Export Citation   CrossMark

ARTICLES YOU MAY BE INTERESTED IN

The Journal
of Chemical Physics

Submit Today

The Emerging Investigators Special Collection and Awards
Recognizing the excellent work of early career researchers!

AIP Publishing

Effects of glassing matrix deuteration on the relaxation properties of hyperpolarized ^{13}C spins and free radical electrons at cryogenic temperatures

Christopher Parish,[1] [ID] Peter Niedbalski,[1,2] Qing Wang,[1] Fatemeh Khashami,[1] Zahra Hayati,[3,4]
Mengtian Liu,[3,4] Likai Song,[3] and Lloyd Lumata[1,a] [ID]

AFFILIATIONS

[1] Department of Physics, University of Texas at Dallas, 800 West Campbell Road, Richardson, Texas 75080, USA
[2] Center for Pulmonary Imaging Research, Cincinnati Children's Hospital Medical Center, 3333 Burnet Avenue,
 Cincinnati, Ohio 45229, USA
[3] National High Magnetic Field Laboratory, Florida State University, Tallahassee, Florida 32306, USA
[4] Department of Physics, Florida State University, Tallahassee, Florida 32306, USA

[a] Author to whom correspondence should be addressed: lloyd.lumata@utdallas.edu

ABSTRACT

Glassing matrix deuteration could be a beneficial sample preparation method for ^{13}C dynamic nuclear polarization (DNP) when large electron paramagnetic resonance (EPR) width free radicals are used. However, it could yield the opposite DNP effect when samples are doped with small EPR width free radicals. Herein, we have investigated the influence of solvent deuteration on the ^{13}C nuclear and electron relaxation that go along with the effects on ^{13}C DNP intensities at 3.35 T and 1.2 K. For ^{13}C DNP samples doped with trityl OX063, the ^{13}C DNP signals decreased significantly when the protons are replaced by deuterons in glycerol:water or DMSO:water solvents. Meanwhile, the corresponding solid-state ^{13}C T_1 relaxation times of trityl OX063-doped samples generally increased upon solvent deuteration. On the other hand, ^{13}C DNP signals improved by a factor of ~1.5 to 2 upon solvent deuteration of samples doped with 4-oxo-TEMPO. Despite this ^{13}C DNP increase, there were no significant differences recorded in ^{13}C T_1 values of TEMPO-doped samples with nondeuterated or fully deuterated glassing matrices. While solvent deuteration appears to have a negligible effect on the electron T_1 relaxation of both free radicals, the electron T_2 relaxation times of these two free radicals generally increased upon solvent deuteration. These overall results suggest that while the solid-phase ^{13}C DNP signals are dependent upon the changes in total nuclear Zeeman heat capacity, the ^{13}C relaxation effects are related to ^{2}H/^{1}H nuclear spin diffusion-assisted ^{13}C polarization leakage in addition to the dominant paramagnetic relaxation contribution of free radical centers.

Published under license by AIP Publishing. https://doi.org/10.1063/1.5096036

I. INTRODUCTION

The strength of the nuclear magnetic resonance (NMR) signal is proportional to the concentration or number of nuclear spins and a parameter known as polarization, which is dictated by Boltzmann statistics.[1–4] At ambient conditions, the surplus number of nuclear spins that contribute to the detectable magnetization is only on the order of a few parts per million.[1] Thus, NMR measurements,

especially for nuclei with a low gyromagnetic ratio (γ) and low natural isotopic abundance in mass-limited samples, can be challenging and even time-consuming. Electrons, on the other hand, can easily acquire large thermal polarization, owing to their relatively large gamma (γ/2π = 28 000 MHz/T), which is three orders of magnitude greater than that of ^{1}H spins (γ/2π = 42.58 MHz/T).[3–5] One manner to improve the NMR sensitivity is to take advantage of the large electron thermal polarization and transfer it to the nuclear spins

via a technique known as dynamic nuclear polarization (DNP).[4,5] Initially invented for the production of highly polarized protons and deuterons in hadron research and nuclear scattering experiments,[4,5] the DNP technique accomplishes this polarization transfer via microwave irradiation of the target sample at cryogenic temperatures and in a high magnetic field. Depending upon the properties of the source of unpaired electrons and other parameters, the DNP process can proceed via solid effect, thermal mixing, cross effect, or a combination thereof.[6–12]

For many decades, this NMR signal amplification technique was confined to or almost exclusively used in nuclear scattering physics experiments[4,5] until the invention of the dissolution DNP method in 2003 by Ardenkjaer-Larsen et al.[13] In dissolution DNP, the cryogenically frozen polarized sample is quickly dissolved with a highly pressured superheated solvent to produce a hyperpolarized liquid at a final temperature tolerable for injection in living systems.[13,14] Using this method,[13] the liquid-state NMR signal has been found to be enhanced by greater than several thousand-fold with respect to the thermal NMR signal for a variety of nuclei with relatively long solution-phase spin-lattice T_1 relaxation times.[15–20] With this capability, dissolution DNP has opened up new avenues of research in chemistry and biomedical imaging especially in *in vitro* and *in vivo* studies of metabolism.[21–29] In particular, it has found application in real-time *in vivo* metabolic magnetic resonance imaging (MRI) for diagnostics of a variety of pathologies.[22–29] Remarkably, this technology has already begun to establish hyperpolarized ^{13}C MRI as a powerful real-time and noninvasive *in vivo* metabolic imaging tool for clinical applications with high biochemical specificity.[28,29]

A variety of factors could affect the maximum achievable NMR or MRI signal enhancements in dissolution DNP.[14,30–32] Instrumental conditions such as a high magnetic field, a lower DNP operating temperature, and faster dissolution liquid transfer could contribute to higher signal enhancements.[30–32] Since DNP involves the interaction of electrons and nuclei, it is also apparent that the nature of the DNP sample composition could have a profound impact on the maximum achievable polarization of the target nuclei.[14,30] In the context of dissolution DNP, a typical DNP sample consists of a compound with the target nuclei (e.g., ^{13}C pyruvate) dissolved in a glassing matrix (e.g., glycerol:water) and doped with trace amounts of free electron sources (e.g., trityl OX063 or TEMPO free radical).[13,14] Previous studies have shown that the maximum achievable NMR enhancements are directly dependent upon the properties of the polarizing agents.[17,33–37] In particular, the narrow electron paramagnetic resonance (EPR) linewidth free radicals such as trityl OX063 appear to yield more favorable DNP results for direct polarization of low-γ nuclei such as ^{13}C spins.[38–42] Other DNP works have demonstrated that not all ^{13}C spins are hyperpolarized with the same efficiency and that the DNP signal is dependent upon the isotopic labeling location of the target nuclei.[43,44] In addition, inclusion of trace amounts of paramagnetic additives such as lanthanides and certain transition metal complexes or nanoparticles in the DNP samples could significantly boost the DNP enhancement.[45–52] Furthermore, isotopic labeling of the other component of the DNP sample, the glassing solvents, could either boost or adversely affect the DNP signal in the frozen state depending upon the EPR linewidth of the free radical polarizing agent used.[53–55] Previous studies[54,55] have found that glassing matrix deuteration could boost the
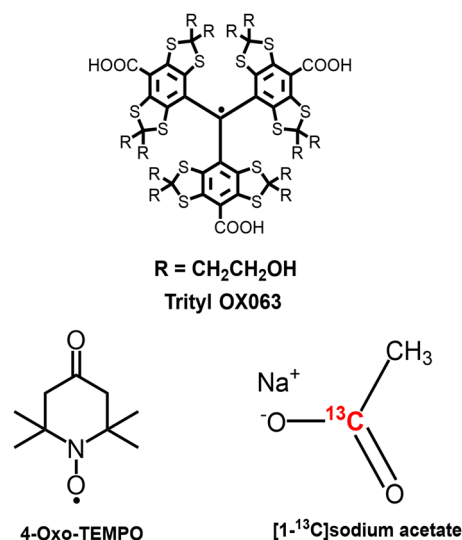

FIG. 1. Structures of the free radicals and ^{13}C-labeled compound used in this study.

^{13}C DNP signal when large EPR linewidth free radicals such as TEMPO are used, whereas the adverse DNP effect is observed when narrow EPR linewidth free radicals such as trityl OX063 or BDPA are used.

While the effects of ^2H enrichment of the glassing matrix on ^{13}C DNP signal intensities are well studied,[53–55] little is known about the concomitant effects of glassing solvent deuteration on the frozen-phase hyperpolarized ^{13}C and free radical relaxation properties under these sample conditions. In this study, we have investigated the influence of ^2H enrichment of the glassing matrix not only on the ^{13}C DNP signal intensities but also on the solid-phase ^{13}C relaxation or depolarization times of hyperpolarized [1-^{13}C] sodium acetate doped with optimum concentration of the narrow EPR linewidth trityl OX063 (15 mM) or the wide EPR width 4-oxo-TEMPO (40 mM) free radical (see the structures in Fig. 1). Furthermore, the electron T_1 and spin-spin T_2 relaxation times of these free radicals at their optimum DNP concentrations were measured using a W-band (95 GHz) pulsed EPR spectrometer. For generality of the measurements, two types of glassing solvents, 1:1 vol/vol glycerol:water and 1:1 v/v dimethyl sulfoxide (DMSO):water, were used. The main goal of this study was to elucidate if the ^{13}C DNP effects observed upon glassing matrix deuteration of the DNP sample are correlated with the changes that occur in the nuclear and electron relaxation properties.

II. EXPERIMENTAL

A. Sample preparation

Chemicals and reagents were purchased commercially and were used without further purification. Three 100 μL aliquots of 3M [1-^{13}C] sodium acetate (Cambridge Isotope Laboratories, Tewksbury, MA) were prepared in 1:1 v/v glycerol:water (Sigma-Aldrich, St. Louis, MO) doped with 15 mM trityl OX063 (Oxford Instruments Biotools, MA).[14] Another set of three 100 μL aliquots were

prepared using the same formulation but this time with 40 mM 4-oxo-TEMPO (Sigma-Aldrich, St. Louis, MO) as the polarizing agent instead of trityl OX063. These two sets of samples were replicated but this time using 1:1 v/v deuterated glycerol:D_2O as the glassing matrix. Thus, a subtotal of 12 samples (triplicates of 4 distinct types of sample formulations) were prepared, with 6 samples in glycerol:water glassing solvents and another 6 samples in deuterated glycerol:D_2O solvents. In addition, 12 100 μL aliquots of DNP samples with the same formulation but with 2M [1-^{13}C] sodium acetate in nondeuterated (ND) and fully deuterated (FD) 1:1 v/v DMSO:water glassing matrices were also prepared. Overall, eight distinct types of DNP samples (trityl OX063 or 4-oxo-TEMPO, glycerol:water or DMSO:water, ND or FD glassing solvents) were prepared in triplicates, yielding a total of 24 ^{13}C DNP samples for this study. Weighing of sample components was done using an Ohaus Discovery semi-micro analytical balance (Ohaus Corporation, NJ). Mixing of the DNP sample solution was done using a BenchMixer V2 vortex mixer (Benchmark Corporation, NJ). All samples were made 4–6 h ahead of the experiment and were stored in a New Brunswick U101 Innova −86 °C ultra-low temperature freezer (Eppendorf, NY) prior to DNP or EPR measurements.

B. DNP measurements

All DNP experiments were performed at the Advanced Imaging Research Center (AIRC) of the University of Texas Southwestern Medical Center (UTSW) using a commercial HyperSense hyperpolarizer (Oxford Instruments, UK). This hyperpolarizer makes use of a 3.35 T superconducting magnet and a Edwards 250 roots blower pump vacuum system (Edwards Vacuum, UK) to bring the base temperature of the cryostat sample space down to 1.2 K.[14] This polarizer is equipped with a 100 mW ELVA microwave source (ELVA-1 Millimeter Wave Division, Russia) that has a variable frequency range of 400 MHz. The optimum microwave frequencies for ^{13}C samples doped with trityl OX063 and 4-oxo-TEMPO are 94.088 GHz and 94.105 GHz, respectively. Using the built-in NMR program in the HyperSense, ^{13}C polarization buildup curves were recorded by applying a train of shallow flip angle radiofrequency (RF) pulses every 3 min until the hyperpolarized signals approached a plateau at 3.35 T and 1.2 K. These buildup curves were fitted with a single exponential buildup $P = P_0(1 - e^{-t/\tau})$ in which P_0 is the maximum relative polarization, t is the microwave irradiation time, and τ is the polarization buildup time. Relative bar graphs of average extrapolated maximum ^{13}C DNP signals ($N = 3$) for each distinct DNP sample type along with their standard deviations were plotted for comparison.

Following the acquisition of ^{13}C buildup polarization curves is the measurement of hyperpolarized ^{13}C NMR signal decay curves from which the solid-phase ^{13}C T_1 relaxation times of the frozen DNP samples can be extracted.[56] The ^{13}C RF coil of the HyperSense was tuned remotely with a series-tuned, parallel-matched capacitor network located outside of the cryostat. This network was connected to a Varian NMRS spectrometer (Agilent Technologies, CA) in order to monitor the hyperpolarized ^{13}C NMR signal decay. This was accomplished by applying a 2° RF pulse every 10 min to the frozen DNP sample until the hyperpolarized ^{13}C NMR signal was less than 5% of its initial amplitude. The hyperpolarized ^{13}C NMR

decay curves were fitted to an exponential decay equation that incorporates the effects of RF pulsing and T_1 relaxation. Solid-phase ^{13}C T_1 values were extracted from these fittings.[17,56] Average values and standard deviations ($N = 3$) of these ^{13}C T_1 values were plotted as bar graphs for comparison.

C. EPR measurements

The EPR measurements of the DNP samples were performed using a W-band (95 GHz) Bruker E680 ESR spectrometer (Bruker Biospin, Billerica, MA) at the National High Magnetic Field Laboratory (NHMFL) in Tallahassee, FL. This EPR spectrometer is equipped with a Bruker TE$_{011}$ cylindrical cavity as well as a CF1200 helium flow cryostat (Oxford Instruments, UK), which was used to control the sample temperature, ranging from 5 K to 300 K. The samples used in EPR measurements were of the same formulation as the ^{13}C DNP samples in this study as described previously. Prior to insertion in the cylindrical cavity, samples were loaded in 0.15 mm ID thin quartz capillary tubes. EPR spectra at 95 GHz were measured for each of the eight distinct ^{13}C DNP samples via a field-swept electron spin-echo method by monitoring Hahn echo intensities at different magnetic fields. The electron T_1 relaxation times of trityl OX063 (15 mM) and 4-oxo-TEMPO (40 mM) in ^{13}C DNP samples were recorded using the saturation recovery method. The ESR saturation recovery curves were fitted with double exponentials such that the resulting longer relaxation time described the electron spin-lattice relaxation time, whereas the shorter time-constant represented the electron-electron cross-relaxation effects.[57,58] In addition, the electron spin-lattice relaxation rates $1/T_1$ of the ^{13}C DNP samples were plotted as a function of temperature from 200 K down to 5 K. Power law fittings on electron $1/T_1$ vs temperature plots were determined to ascertain the electron relaxation mechanisms on various temperature ranges. Furthermore, electron T_2 transverse relaxation times were also measured using the standard Hahn echo decay technique. The results were plotted as bar graphs for comparison.

D. Data analyses

All DNP-NMR and EPR data were analyzed and graphed using Igor Pro version 7.081 (WaveMetrics, OR). The hyperpolarized ^{13}C NMR signal decay data obtained from the Varian VNMRS spectrometer were analyzed using ACD Lab version 12 (Advanced Chemistry Development, Toronto, Canada). Average values and standard deviations were calculated for experiments with $N = 3$ trials.

III. RESULTS AND DISCUSSION

The narrow EPR width free radical trityl OX063 is one of the most effective polarizing agents for dissolution DNP of ^{13}C-labeled compounds and other samples with low-γ nuclei.[38–42] At DNP conditions of 3.35 T and temperatures close to 1 K at which the HyperSense polarizer is operating, the predominant DNP mechanism for trityl OX063-doped ^{13}C DNP samples appears to be the thermal mixing process.[17,20,42] Thermal mixing is the dominant DNP process when the nuclear Larmor frequency is comparable to or less than the EPR linewidth of the free radical polarizing agent.[4,5,10] In this DNP mechanism, the energy of the electron dipolar system (EDS) is

comparable to the energy of the nuclear Zeeman system (NZS); thus, a thermal contact can be established between the two systems.[4,5] Microwave irradiation of the DNP sample at slightly off EPR resonant frequency of the free radical can lead to dynamic cooling of EDS, which in turn cools or lowers the spin temperature of NZS.[10] Thus, the two thermodynamic reservoirs EDS and NZS eventually acquire the same lower spin temperature which implies that the nuclear polarization is enhanced far from the thermal equilibrium spin distribution.[7,10] Furthermore, multiple nuclear Zeeman reservoirs can come into thermal contact with a common electron spin-spin interaction reservoir under thermal mixing conditions.[59–62] In turn, this common link with EDS allows the various nuclear Zeeman reservoirs to establish thermal contact with each other.[60–62] In such cases, a single EDS will have to cool multiple NZS and thus the total nuclear Zeeman heat load could affect the final spin temperature of these polarized nuclei. It should be noted that the heat capacity of the nuclear Zeeman reservoir in the thermal mixing regime can be approximated by $C_{NZ} \sim N(\gamma B_{loc})^2$, where N is the number of nuclear spins and B_{loc} is the local magnetic field.[10]

The ^{13}C DNP behavior displayed in Fig. 2(a) can be explained by these thermodynamic arguments. As seen in the relative polarization buildup curves and bar graphs in Fig. 2(a), there is a significant reduction of about 30%–50% of the original maximum ^{13}C DNP intensity when the glycerol:water or DMSO:water glassing solvents were replaced by their deuterated counterparts. When the ^{13}C spins ($\gamma/2\pi = 10.71$ MHz/T) are in the nondeuterated (ND) glassing solvents, the trityl OX063 EDS is only in thermal contact with ^{13}C NZS; the ^{1}H EDS is decoupled from the trityl OX063 EDS because the ^{1}H Larmor frequency is significantly greater than the trityl EPR linewidth.[54,55] Now, when ^{1}H spins ($\gamma/2\pi = 42.58$ MHz/T) in the glassing matrix are replaced by ^{2}H spins ($\gamma/2\pi = 6.54$ MHz/T), the trityl OX063 EDS is in thermal contact not only with the ^{13}C NZS but also with ^{2}H NZS.[55] This means that the NZS heat load for the EDS to cool has now increased because of additional thermal

coupling with the ^{2}H spins.[10,55] Consequently, this leads to a decrease in the solid-phase ^{13}C DNP signals of samples with deuterated glassing solvents, as seen in Fig. 2(a).

While a reduction effect in ^{13}C DNP intensities of trityl OX063-doped samples was observed upon deuteration of the glassing solvents, the solid-phase ^{13}C T_1 relaxation times reveal a different story. Before delving into the details, it should be noted that the "effective" solid-state ^{13}C T_1 relaxation times described here refer to the depolarization time or decay rate of the hyperpolarized ^{13}C NMR signal which can be ascribed to a number of physical factors, some of which are exclusive to a hyperpolarized sample. In Fig. 2(b), significant increases in the solid-phase ^{13}C T_1 relaxation times were recorded in samples with ^{2}H-enriched glassing solvents. In particular, the ^{13}C T_1 of trityl OX063-doped [1-^{13}C] acetate sample in glycerol:H$_2$O doubled from about 8000 s to 16 000 s when deuterated glycerol:D$_2$O was used as the glassing solvent at 3.35 T and 1.2 K. On the other hand, the solid-state ^{13}C T_1 increased from 9000 s to 15 000 s when the glassing matrix was changed from ND to FD versions of DMSO:water. At 1.2 K, the nuclear spins of the frozen polarized samples relax essentially through the paramagnetic effect induced by the free radical electrons.[4,63,64] The aforementioned trityl OX063-doped ^{13}C DNP samples, however, were all doped with the same optimum concentration of the free radical (15 mM). Thus, the solid-phase ^{13}C T_1 differences observed in samples with ND and FD glassing matrices in Fig. 2(a) can be attributed almost exclusively to the isotopic changes in the glassing matrices. A possible explanation of the solid-state ^{13}C T_1 elongation upon glassing matrix deuteration is that ^{13}C polarization can leak toward the surrounding nuclei via nuclear spin diffusion,[59] which is still active after the microwave irradiation was turned off. Since $\gamma(^2$H$) < \gamma(^1$H$)$, spin diffusion-assisted leakage of ^{13}C polarization is less efficient in ^{13}C DNP samples with deuterated glassing matrices; thus, the ^{13}C polarization decay is slower. Longer solid-state ^{13}C T_1 relaxation is generally considered as a beneficial characteristic of a DNP sample because it translates
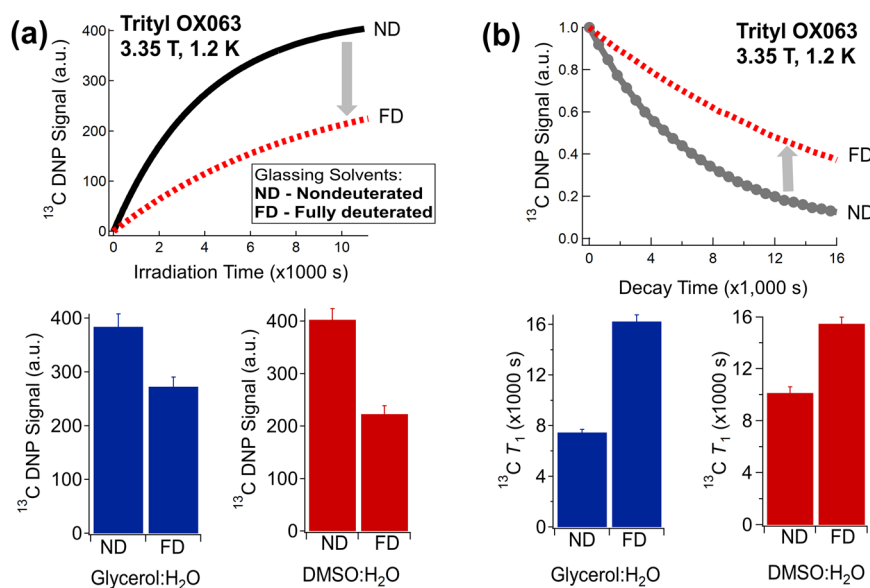

FIG. 2. Effect of glassing solvent deuteration on trityl OX063-doped ^{13}C DNP samples at 3.35 T and 1.2 K: (a) *Top*: Representative ^{13}C DNP buildup curves for ^{13}C samples with nondeuterated (ND) and fully deuterated (FD) glassing solvents. *Bottom*: Comparative bar graphs of extrapolated ^{13}C DNP intensities for ND and FD glycerol:H$_2$O or DMSO:H$_2$O glassing solvents. (b) *Top*: Representative hyperpolarized ^{13}C T_1 decay curves for ^{13}C samples with ND and FD solvents. Bottom: Relative bar graphs of ^{13}C T_1 values of frozen ^{13}C DNP samples with ND and FD glassing solvents.

to longer preservation time of the hyperpolarized state of the ^{13}C spins at cryogenic temperatures.[43,65] Our data however suggest that the solid-phase ^{13}C DNP signal and effective ^{13}C T_1 relaxation time upon ^{2}H enrichment of the glassing matrix for trityl-doped ^{13}C samples do not correlate with one another. This is in contrast to the results of a previous study in which there is a correlation of the maximum solid-phase ^{13}C DNP signals and ^{13}C T_1 relaxation times upon intramolecular isotopic substitutions in acetate.[43]

On the other hand, the solid-phase ^{13}C DNP signal and depolarization data (see Fig. 3) using 4-oxo-TEMPO as the polarizing agent reveal different behavior compared to the trityl OX063 results. The behavior changes because the EPR width of 4-oxo-TEMPO is larger than the ^{1}H Larmor frequency at the DNP conditions of 3.35 T and 1.2 K, and thus the ^{1}H NZS is now thermally coupled to TEMPO EDS in addition to the low-γ NZS such as that of ^{13}C and ^{2}H spins.[53–55] This means that in the ^{13}C DNP samples with ND glassing solvents, the total nuclear Zeeman heat load for TEMPO EDS to cool is a composite of ^{1}H + ^{13}C NZS. When the FD versions of the glassing solvents are used, the TEMPO EDS has to cool ^{2}H + ^{13}C NZS which is a lesser heat load than ^{1}H + ^{13}C due to the lower gamma of ^{2}H spins compared to ^{1}H spins. As a result, ^{13}C NZS can acquire a lower spin temperature with deuterated glassing solvents which explains the significant improvement in the solid-phase ^{13}C DNP signal intensities, as shown in Fig. 3(a).[53,55] This ^{13}C DNP signal improvement was seen in ^{2}H enrichment of glycerol:water and DMSO:water glassing solvents, indicating the generality of the ^{13}C DNP behavior.

While drastic improvements in ^{13}C DNP signals are observed in ^{2}H-enriched glassing solvents of TEMPO-doped DNP samples, the corresponding solid-state effective ^{13}C T_1 relaxation times of these samples did not show any significant differences when ND and FD glassing solvents are used, as shown in Fig. 3(b). For TEMPO-doped ^{13}C samples in glycerol:water, the ^{13}C T_1 was about 4000 s with ND or FD glassing solvents at 3.35 T and 1.2 K. A slight but nonstatistically significant increase from about 2750 s to 3000 s

was recorded for solid-phase ^{13}C T_1 when the DMSO:H$_2$O glassing solvent was switched from ND to FD. A possible explanation for this behavior would be that 4-oxo-TEMPO provides an efficient relaxation mechanism for all nuclear spins in the sample because of its EPR width that is larger than the Zeeman resonance frequencies of the various nuclei present in the sample,[55] which quenches part of the nuclear spin diffusion leakage and makes relaxation the main process of polarization loss. We also note that 4-oxo-TEMPO has a relatively high optimum DNP concentration of 40 mM compared to trityl which is optimal for DNP samples at 15 mM.[17] Nevertheless, the ^{13}C DNP pattern observed for TEMPO-doped samples with ^{2}H-enriched solvents does not correlate with the depolarization behavior at the optimum DNP concentration of this free radical. Thus, these data support the notion that the improvement seen in ^{13}C DNP signals in TEMPO-doped samples with ^{2}H-enriched solvents can be ascribed mainly to the reduction of the total nuclear Zeeman heat load[53,55] as opposed to changes in nuclear relaxation.

Next, we have also investigated the possible effects of ^{2}H enrichment of glassing solvents on the EPR properties of the free radical polarizing agents trityl OX063 (15 mM) and 4-oxo-TEMPO (40 mM) at W-band, as shown in Fig. 4. The EPR spectra and electron relaxation times are important factors to consider in DNP since these parameters can affect the maximum achievable nuclear polarization in the context of equal spin temperature model of DNP.[4,7] As such, any changes in these parameters that might arise with ^{2}H enrichment of the glassing matrix might also affect the DNP signal. In fact, the reduction of electron T_1 of free radicals like trityl OX063 due to inclusion of lanthanides or transition metals in DNP samples is intimately linked to the improvement observed in ^{13}C DNP signal intensities as reported in previous studies.[45–52] In this study, the same formulation of ^{13}C DNP samples was used for EPR measurements to ascertain the actual behavior of electrons under DNP conditions. Our results in Fig. 4(a) show that ^{2}H-enrichment of the glassing matrix in trityl OX063-doped samples did not produce
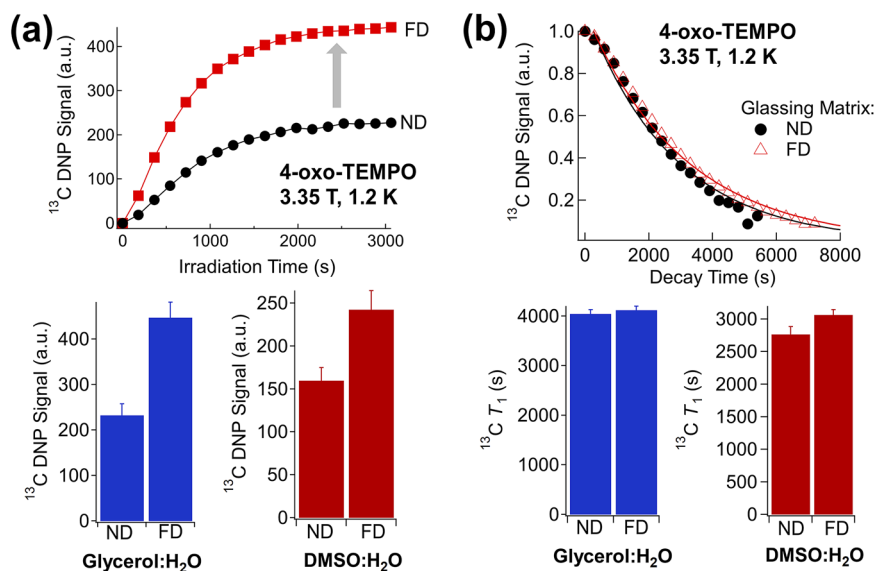

FIG. 3. Influence of glassing solvent deuteration on ^{13}C DNP samples doped with 4-oxo-TEMPO free radical: (a) *Top*: Representative ^{13}C DNP buildup curves for ^{13}C samples with nondeuterated (ND) and fully deuterated (FD) glassing solvents. *Bottom*: Comparative bar graphs of ^{13}C DNP intensities for ND and FD glycerol:H$_2$O or DMSO:H$_2$O glassing solvents. (b) *Top*: Representative hyperpolarized ^{13}C T_1 decay curves for ^{13}C samples with ND and FD solvents. Bottom: Relative bar graphs of ^{13}C T_1 values of frozen ^{13}C DNP samples with ND and FD solvents. Mean values ($N = 3$) and standard deviations of ^{13}C DNP signals and ^{13}C T_1 values are displayed. All these DNP measurements were taken at 3.35 T and 1.2 K.
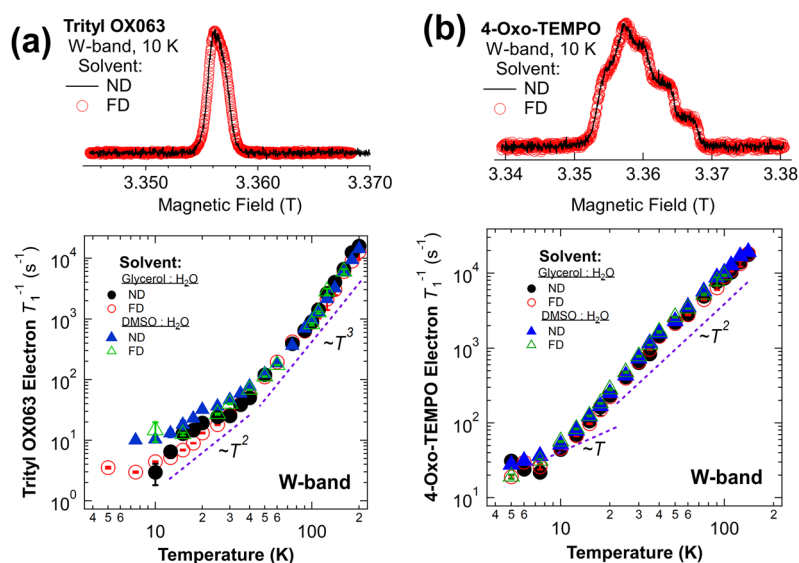
FIG. 4. W-band EPR measurements of ^{13}C DNP samples: (a) *Top*: Representative EPR spectra of trityl OX063 with ND and FD glassing solvents. *Bottom*: Temperature dependence of trityl OX063 electron spin-lattice relaxation rate ($1/T_1$) for ^{13}C DNP samples with ND and FD glycerol:H_2O or DMSO:H_2O glassing matrices. (b) *Top*: Representative EPR spectra of 4-oxo-TEMPO in ND and FD solvents. *Bottom*: 4-Oxo-TEMPO electron T_1 relaxation rates vs temperature in ND and FD glassing solvents. The dashed lines denote the apparent temperature power-law dependence of electron $1/T_1$.

any significant changes in the EPR spectrum compared to the EPR signal in the ND solvent. Furthermore, the temperature-dependent electron spin-lattice relaxation rates $1/T_1$ of trityl OX063 basically overlap with each other when ND or FD glassing solvents are used. There was a slight difference seen between the trityl OX063 electron relaxation rates in glycerol:water and DMSO:water, albeit not significant, in the low temperature region below 15 K. For both solvents, the trityl OX063 electron $1/T_1$ approximately varies according to T^3 in the temperature range 40–200 K which suggests that the predominant relaxation process in this regime is the multiple-phonon Orbach process[66] and possibly a combination of other relaxation mechanisms. In the temperature range 10–40 K, the trityl OX063 electron relaxation rate approximately follows a T^2 dependence, which implies that the two-phonon Raman process[66] is the dominant relaxation contribution. Below 10 K, the electron relaxation rates are either almost linear with or independent of temperature which suggests that the one-phonon direct process[36,66,67] is the foremost electron relaxation mechanism. In Fig. 4(b), the EPR spectra of 4-oxo-TEMPO at optimal DNP doping reveal no difference between samples with ND or FD glassing matrices. In addition, no significant changes were observed in 4-oxo-TEMPO electron $1/T_1$ vs T curves. In fact, the 4-oxo-TEMPO relaxation rates in four different or distinct glassing solvents overlap with each other across the 5–200 K temperature range. Due to relatively higher optimum concentration in DNP samples, 4-oxo-TEMPO exhibits a relatively faster electron relaxation rate than trityl OX063 across the entire temperature range in this study. The electron relaxation mechanism for 4-oxo-TEMPO between 10 and 200 K appears to be predominantly the Raman process, while it becomes primarily temperature-independent below 10 K indicative of the direct process.[66,67] In sum, replacement of ^{1}H spins by ^{2}H spins in the glassing solvents does not seem to significantly affect the EPR spectra and electron T_1 relaxation of both trityl OX063 and 4-oxo-TEMPO free radicals at their optimum DNP concentrations.

Although the electron T_1 relaxation times of both free radicals are unaffected by ^{2}H enrichment of the glassing matrix, a different behavior is observed for the electron T_2 transverse or spin-spin relaxation times. As seen in the representative transverse magnetization dephasing or decay curves in Fig. 5(a), the trityl OX063 electron T_2 relaxation time at W-band and 5 K is significantly elongated by almost a factor of 2 upon deuteration of the glycerol:water glassing matrix. Figure 5(b) shows the generality of this electron T_2 elongation behavior for both trityl OX063 and 4-oxo-TEMPO free radicals when the ND glassing solvents are switched to their FD counterparts. These electron T_2 relaxation results are reminiscent of the deuteration effects on electron spin echo dephasing times T_m for EPR distance measurements in proteins or enzymes.[68,69] As reported in previous works,[68–70] ^{2}H enrichment of proteins and/or the solvents can increase the T_m values of the spin labels such as nitroxides. This behavior, which is beneficial for increasing the sensitivity and range of distances that can be measured with site-selective spin labels by EPR, is ascribed to the reduced dipolar interaction between the unpaired electrons and the surrounding coupled ^{1}H spins in the proteins and the solvents.[68] The large number of dipolar-coupled ^{1}H spins in these surrounding environments makes ^{1}H nuclear spin flips or spin diffusion more probable, which is an effective mechanism in dephasing electron spins.[68,70] Since ^{2}H spins have smaller magnetic moments than ^{1}H spins, nuclear spin diffusion is less effective for deuterons; thus, the T_m values of the spin label are elongated under this condition. In this study, we invoke the same physical explanation for the increase in electron T_2 relaxation times of the free radicals in deuterated glassing conditions. Although electron T_1 appears to be a more relevant EPR parameter in determining the DNP efficiency, electron T_2 is embedded in DNP-related parameters such as the nuclear relaxation induced by free electrons[63,64] and the energy-conserving electron flip-flop[4] that accompanies a nuclear spin flip during DNP. It is worthwhile to note that the dephasing times of free radical electrons can be significantly altered
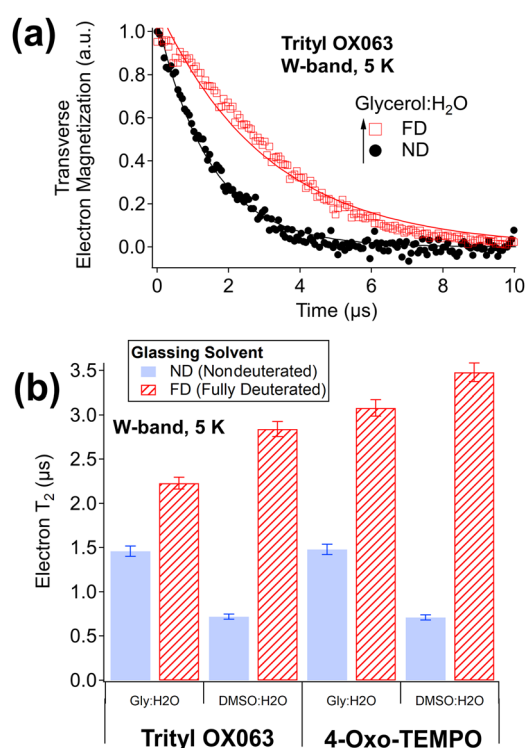
FIG. 5. (a) Representative electron T_2 transverse magnetization dephasing curves for trityl OX063 in ND and FD glycerol:water solvents at W-band and 5 K. The solid curves are fits to an exponential decay equation. (b) Bar graphs showing the increase in electron T_2 values of trityl OX063 and 4-oxo-TEMPO at W-band and 5 K upon deuteration of the glassing solvents.

by the isotopic substitutions in the glassing solvents under DNP conditions.

IV. CONCLUSION

In conclusion, we have investigated, for the first time, the effects of replacing ^1H spins with ^2H spins in the glassing solvents on the relaxation properties of hyperpolarized ^{13}C spins and free radical electrons that go along with the changes that occur in ^{13}C DNP signal intensities at cryogenic temperatures. Our results indicate that for ^{13}C DNP samples doped with narrow EPR width trityl OX063, the solid-phase ^{13}C T_1 relaxation or depolarization times are significantly increased, while the ^{13}C DNP signals are reduced to about a half upon ^2H isotopic enrichment of the glassing matrices. The decrease in ^{13}C DNP intensity for trityl OX063-doped samples is attributed to increased nuclear Zeeman heat load due to thermal link of electron spin-spin interaction reservoir with both ^2H and ^{13}C nuclear Zeeman reservoirs. Meanwhile, the increase in ^{13}C T_1 relaxation or depolarization times is ascribed to the reduced nuclear spin diffusion-assisted leakage of ^{13}C polarization when ^1H spins are replaced by ^2H spins in the glassing matrices. In addition, the EPR spectra and electron T_1 relaxation times of trityl OX063 remained unchanged when the glassing solvents are deuterated. On the other hand, the ^{13}C DNP signal improves significantly when the wide EPR

width 4-oxo-TEMPO free radical is used, and this is ascribed to the reduction in total nuclear Zeeman heat load when the high-gamma protons are substituted with low-gamma deuterons in the glassing solvents. In spite of the ^{13}C DNP signal increase in TEMPO-doped samples, the ^{13}C T_1 relaxation times remained unchanged when deuterated solvents are used. This is ascribed to the fact that the TEMPO EPR width is larger than the nuclear Larmor frequencies of the various nuclei present in the sample, which quenches part of the nuclear spin diffusion leakage and makes paramagnetic relaxation contribution the dominant source of ^{13}C polarization loss. Similar to trityl OX063 results, there were no significant differences in the EPR spectra and electron T_1 relaxation times of 4-oxo-TEMPO when the glassing solvents are switched to their deuterated counterparts. The electron T_2 relaxation times for both free radicals, however, are drastically increased in deuterated glassing solvents. This electron T_2 behavior is attributed to less effective nuclear spin flips or spin diffusion when ^1H spins are replaced with ^2H spins in the solvents. These overall results indicate that the relative ^{13}C DNP intensities might be decoupled or less affected from the changes that occur in the nuclear relaxation due to solvent deuteration. Overall, these experimentally measured relaxation parameters have provided some insights into the dynamical behavior of nuclear and electron spins under nondeuterated and deuterated solvent environments at DNP conditions.

REFERENCES

[1] M. H. Levitt, *Spin Dynamics: Basics of Nuclear Magnetic Resonance*, 2nd ed. (John Wiley & Sons, Ltd., West Sussex, 2008).

[2] C. P. Slichter, *Principles of Magnetic Resonance*, 3rd ed. (Springer-Verlag, Berlin, 1990).

[3] A. Abragam, *The Principles of Nuclear Magnetism* (Clarendon Press, Oxford, 1961).

[4] A. Abragam and M. Goldman, Rep. Prog. Phys. **41**, 395 (1978).

[5] D. G. Crabb and W. Meyer, Annu. Rev. Nucl. Part. Sci. **47**, 67 (1997).

[6] W. T. Wenckebach, Appl. Magn. Reson. **34**, 227 (2008).

[7] M. Borghini, Phys. Rev. Lett. **20**, 419 (1968).

[8] W. T. Wenckebach, J. Magn. Reson. **277**, 68 (2017).

[9] Y. Hovav, A. Feintuch, and S. Vega, J. Magn. Reson. **214**, 29 (2012).

[10] S. T. Goertz, Nucl. Instrum. Methods Phys. Res., Sect. A **526**, 28 (2004).

[11] W. T. Wenckebach, J. Magn. Reson. **299**, 124 (2019).

[12] D. Shimon, Y. Hovav, A. Feintuch, D. Goldfarb, and S. Vega, Phys. Chem. Chem. Phys. **14**, 5729 (2012).

[13] J. H. Ardenkjaer-Larsen, B. Fridlund, A. Gram, G. Hansson, L. Hansson, M. H. Lerche, R. Servin, M. Thaning, and K. Golman, Proc. Natl. Acad. Sci. U. S. A. **100**, 010158 (2003).

[14]L. Lumata, C. Yang, M. Ragavan, N. Carpenter, R. J. DeBerardinis, and M. E. Merritt, Methods Enzymol. **561**, 73 (2015).

[15]W. Jiang, L. Lumata, W. Chen, S. Zhang, Z. Kovacs, A. D. Sherry, and C. Khemtong, Sci. Rep. **5**, 9104 (2015).

[16]L. Lumata, M. E. Merritt, C. Malloy, A. D. Sherry, and Z. Kovacs, Appl. Magn. Reson. **43**, 69 (2012).

[17]L. Lumata, A. K. Jindal, M. E. Merritt, C. R. Malloy, A. D. Sherry, and Z. Kovacs, J. Am. Chem. Soc. **133**, 8673 (2011).

[18]L. Lumata, M. E. Merritt, Z. Hashami, S. J. Ratnakar, and Z. Kovacs, Angew. Chem., Int. Ed. **51**, 525 (2012).

[19]R. Balzan, M. Mishkovsky, Y. Simonenko, R. B. van Heeswijk, R. Gruetter, U. Eliav, G. Navon, and A. Comment, Contrast Media Mol. Imaging **11**, 41 (2016).

[20]S. Reynolds and H. Patel, Appl. Magn. Reson. **34**, 495 (2008).

[21]K. R. Keshari and D. M. Wilson, Chem. Soc. Rev. **43**, 1627 (2014).

[22]J. Kurhanewicz, D. B. Vigneron, K. Brindle, E. Y. Chekmenev, A. Comment, C. H. Cunningham, R. J. DeBerardinis, G. G. Green, M. O. Leach, S. S. Rajan, R. R. Rizi, B. D. Ross, W. S. Warren, and C. R. Malloy, Neoplasia **13**, 81 (2011).

[23]F. A. Gallagher, M. I. Kettunen, and K. M. Brindle, Prog. Nucl. Magn. Reson. Spectrosc. **55**, 285 (2009).

[24]K. M. Brindle, S. E. Bohndiek, F. A. Gallagher, and M. I. Kettunen, Magn. Reson. Med. **66**, 505 (2011).

[25]K. M. Brindle, J. Am. Chem. Soc. **137**, 6418 (2015).

[26]C. Yang, B. Ko, C. Hensley, L. Jiang, A. Wasti, L. Lumata, M. Mitsche, M. Merritt, and R. J. DeBerardinis, Mol. Cell **56**, 414–424 (2014).

[27]C. Khemtong, N. R. Carpenter, L. L. Lumata, M. E. Merritt, K. X. Moreno, Z. Kovacs, C. R. Malloy, and A. D. Sherry, Magn. Reson. Med. **74**, 312 (2015).

[28]S. J. Nelson, J. Kurhanewicz, D. B. Vigneron, P. E. Z. Larson, A. L. Harzstark, M. Ferrone, M. van Criekinge, J. W. Chang, R. Bok, I. Park, G. Reed, L. Carvajal, E. J. Small, P. Munster, V. K. Weinberg, J. H. Ardenkjaer-Larsen, A. P. Chen, R. E. Hurd, L.-I. Odegardstuen, F. J. Robb, J. Tropp, and J. A. Murray, Sci. Transl. Med. **5**, 198ra108 (2013).

[29]C. H. Cunningham, J. Y. Lau, A. P. Chen, B. J. Geraghty, W. J. Perks, I. Roifman, G. A. Wright, and K. A. Connelly, "Hyperpolarized ^{13}C metabolic MRI of the human heart: Initial experience," Circ. Res. **119**, 1177 (2016).

[30]P. Niedbalski, A. Kiswandhi, C. Parish, Q. Wang, F. Khashami, and L. Lumata, J. Phys. Chem. Lett. **9**, 5481 (2018).

[31]J. H. Ardenkjaer-Larsen, J. Magn. Reson. **264**, 3 (2016).

[32]F. Jähnig, G. Kwiatkowski, and M. Ernst, J. Magn. Reson. **264**, 22 (2016).

[33]L. Lumata, S. J. Ratnakar, A. Jindal, M. Merritt, A. Comment, C. Malloy, A. D. Sherry, and Z. Kovacs, Chem. – Eur. J. **17**, 10825 (2011).

[34]L. Lumata, M. Merritt, C. Khemtong, S. J. Ratnakar, J. van Tol, L. Yu, L. Song, and Z. Kovacs, RSC Adv. **2**, 12812 (2012).

[35]L. L. Lumata, M. E. Merritt, C. R. Malloy, A. D. Sherry, J. van Tol, L. Song, and Z. Kovacs, J. Magn. Reson. **227**, 14 (2013).

[36]L. Lumata, Z. Kovacs, A. D. Sherry, C. Malloy, S. Hill, J. van Tol, L. Yu, L. Song, and M. E. Merritt, Phys. Chem. Chem. Phys. **15**, 9800 (2013).

[37]A. Comment, B. van den Brandt, K. Uffmann, F. Kurdzesau, S. Jannin, J. A. Konter, P. Hautle, W. T. Wenckebach, R. Gruetter, and J. J. van der Klink, Concepts Magn. Reson., Part B **31B**, 255 (2007).

[38]L. L. Lumata, R. Martin, A. K. Jindal, Z. Kovacs, M. S. Conradi, and M. E. Merritt, Magn. Reson. Mater. Phys., Biol. Med. **28**, 195 (2015).

[39]A. Kiswandhi, P. Niedbalski, Q. Wang, C. Parish, and L. Lumata, Magn. Reson. Chem. **55**, 846 (2017).

[40]A. Kiswandhi, P. Niedbalski, C. Parish, S. Ferguson, D. Taylor, G. McDonald, and L. Lumata, Magn. Reson. Chem. **55**, 828 (2017).

[41]H. A. I. Yoshihara, E. Can, M. Karlsson, M. H. Lerche, J. Schwitterd, and A. Comment, Phys. Chem. Chem. Phys. **18**, 12409 (2016).

[42]J. Wolber, F. Ellner, B. Fridlund, A. Gram, H. Jóhannesson, G. Hansson, L. H. Hansson, M. H. Lerche, S. Månsson, R. Servin, M. Thaning, K. Golman,

and J. H. Ardenkjær-Larsen, Nucl. Instrum. Methods Phys. Res., Sect. A **526**, 173 (2004).

[43]P. Niedbalski, C. Parish, A. Kiswandhi, Z. Kovacs, and L. Lumata, J. Phys. Chem. A **121**, 3227 (2017).

[44]C. Parish, P. Niedbalski, A. Kiswandhi, and L. Lumata, J. Chem. Phys. **149**, 054302 (2018).

[45]J. W. Gordon, S. B. Fain, and I. J. Rowland, Magn. Reson. Med. **68**, 1949 (2012).

[46]L. Friesen-Waldner, A. Chen, W. Mander, T. J. Scholl, and C. A. McKenzie, J. Magn. Reson. **223**, 85 (2012).

[47]A. A. Sirusi, E. H. Suh, Z. Kovacs, and M. E. Merritt, Phys. Chem. Chem. Phys. **20**, 728 (2018).

[48]P. Niedbalski, C. Parish, A. Kiswandhi, L. Fidelino, C. Khemtong, Z. Hayati, L. Song, A. Martins, A. D. Sherry, and L. Lumata, J. Chem. Phys. **146**, 014303 (2017).

[49]A. Kiswandhi, P. Niedbalski, C. Parish, P. Kaur, A. Martins, L. Fidelino, C. Khemtong, L. Song, A. D. Sherry, and L. Lumata, Phys. Chem. Chem. Phys. **18**, 21351 (2016).

[50]P. Niedbalski, C. Parish, Q. Wang, A. Kiswandhi, Z. Hayati, L. Song, and L. Lumata, J. Phys. Chem. A **121**, 5127 (2017).

[51]P. Niedbalski, C. Parish, Q. Wang, Z. Hayati, L. Song, A. F. Martins, A. D. Sherry, and L. Lumata, J. Phys. Chem. A **121**, 9221 (2017).

[52]P. Niedbalski, C. R. Parish, Q. Wang, Z. Hayati, L. Song, Z. I. Cleveland, and L. Lumata, J. Phys. Chem. C **121**, 19505 (2017).

[53]F. Kurdzesau, B. van den Brandt, A. Comment, P. Hautle, S. Jannin, J. J. van der Klink, and J. A. Konter, J. Phys. D: Appl. Phys. **41**, 155506 (2008).

[54]A. Kiswandhi, B. Lama, P. Niedbalski, M. Goderya, J. Long, and L. Lumata, RSC Adv. **6**, 38855 (2016).

[55]L. Lumata, M. E. Merritt, and Z. Kovacs, Phys. Chem. Chem. Phys. **15**, 7032 (2013).

[56]B. R. Patyal, J. H. Gao, R. F. Williams, J. Roby, B. Saam, B. A. Rockwell, R. J. Thomas, D. J. Stolarski, and P. T. Fox, J. Magn. Reson. **126**, 58 (1997).

[57]C. T. Farrar, D. A. Hall, G. J. Gerfen, S. J. Inati, and R. G. Griffin, J. Chem. Phys. **114**, 4922 (2001).

[58]T. A. Siaw, M. Fehr, A. Lund, A. Latimer, S. A. Walker, D. T. Edwards, and S.-I. Han, Phys. Chem. Chem. Phys. **16**, 18694 (2014).

[59]T. Wenckebach, *Essentials of Dynamic Nuclear Polarization* (Spindrift Publications, The Netherlands, 2016).

[60]W. de Boer, M. Borghini, K. Morimoto, T. O. Niinikoski, and F. Udo, J. Low Temp. Phys. **15**, 249 (1974).

[61]S. F. J. Cox, V. Bouffard, and M. Goldman, J. Phys. C: Solid State Phys. **6**, L100 (1973).

[62]E. Guarin, S. Marhabaie, A. Rosso, D. Abergel, G. Bodenhausen, K. L. Ivanov, and D. Kurzbach, J. Phys. Chem. Lett. **8**, 5531 (2017).

[63].J. H. Ardenkjær-Larsen, S. Macholl, and H. Johanesson, Appl. Magn. Reson. **34**, 509 (2008).

[64]A. Abragam and M. Goldman, *Nuclear Magnetism: Order and Disorder* (Clarendon Press, Oxford, 1982).

[65]P. Niedbalski, Q. Wang, C. Parish, F. Khashami, A. Kiswandhi, and L. Lumata, J. Phys. Chem. B **122**, 1898 (2018).

[66]A. Abragam and B. Bleaney, *Electron Paramagnetic Resonance of Transition Ions* (Oxford University Press, Oxford, 2012).

[67]K. N. Shrivastava, Phys. Status Solidi B **117**, 437 (1983).

[68]E. M. Hassane, R. Ward R, A. Bowman, T. Owen-Hughes, and D. G. Norman, J. Magn. Reson. **248**, 36 (2014).

[69]R. Ward, A. Bowman, E. Sozudogru, H. El-Mkami, T. Owen Hughes, and D. G. Norman, J. Magn. Reson. **207**, 164 (2010).

[70]P. P. Borbat and J. H. Freed, Methods Enzymol. **423**, 52 (2007).